11 WCEE

Copyright © 1996 Elsevier Science Ltd
Paper No. 1097. (quote when citing this article)
Eleventh World Conference on Earthquake Engineering
ISBN: 0 08 042822 3

A NEW APPROACH TO EVALUATE POST-LIQUEFACTION PERMANENT DEFORMATION IN SATURATED SAND

Yasuhiro SHAMOTO, Jian-Min ZHANG and Sigeru GOTO
Institute of Technology, Shimizu Corporation, 4-17, Etchujima 3-Chome, Tokyo

Kohji TOKIMATSU
Tokyo Institute of Technology, 12-1, O-okayama 2-Chome, Tokyo

ABSTRACT

The post-liquefaction deformation may be classified into volumetric deformation due to reduction in soil volume and deviator deformation due to a shearing application. In this study, both of them are described using the new constitutive relations proposed by the authors. A simplified method is then presented to estimate post-liquefaction permanent lateral displacements and settlements in saturated sand deposits. The effectiveness of the proposed method is checked favorably with the actual observations during the 1995 Hyogo-ken Nanbu earthquake.

KEYWORDS

post-liquefaction; ground settlement; lateral permanent ground displacement; saturated sand.

INTRODUCTION

Post-liquefaction permanent ground deformation occurred and caused heavy damage to various structures, for example, during the 1964 Niigata earthquake and the 1995 Hyogo-ken Nanbu earthquake (e.g., Hamada *et al.*, 1986). Such ground displacements may occur even in deposits with nearly level ground. Therefore, probable ground deformation should be properly evaluated in the design of various structures founded on liquefiable soil deposits.

The post-liquefaction deformation may be divided into volumetric deformation that induces ground settlement and deviator deformation that causes lateral ground displacement. The ground settlement can be evaluated approximately using the simplified methods such as those proposed by Tokimatsu & Seed (1987) and Ishihara & Yoshimine (1992) as well as by Shamoto *et al.* (1995a). However, no method has been considered to be reasonable for predicting the lateral ground displacement, although several studies have been done.

The object of this paper is to present a new approach to predict liquefaction-induced permanent deformation, including ground settlement and lateral displacement, in sandy soil deposits with either level or inclined surfaces. The proposed method is confirmed to be effective as a first approximation for the above subject.

POST-LIQUEFACTION VOLUME CHANGE AND RELATIVE COMPRESSION

The phenomenon that the effective stress state becomes zero for the first time in saturated sand subjected to cyclic undrained loading was termed "initial liquefaction" (Seed & Lee, 1966), which may separate pre- and post-liquefaction conditions in time domain. Tests show that the pre- and post-liquefaction behavior of saturated sands exhibit quite different. The term "post-liquefaction" used in this study indicates the undrained response of sands to either cyclic or monotonic loading after initial liquefaction.

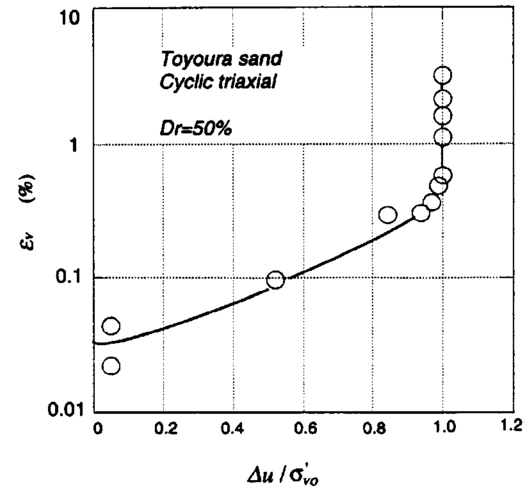

Fig.1 Relationship between induced excess pore pressure ratio and corresponding drained volumetric strain

Fig. 1 shows the relationship between excess pore pressure ratio $\Delta u/\sigma'_{vo}$ induced by cyclic undrained loading and residual volumetric strain ε_{vr} due to subsequent isotropic consolidation (Shamoto, *et al.*, 1995c). It is found that the value of ε_{vr} is well correlated with $\Delta u/\sigma'_{vo}$ when $\Delta u/\sigma'_{vo}$ is less than 100%, but that it shows a very large scatter when $\Delta u/\sigma'_{vo}$ reaches 100%. It is therefore difficult to evaluate post-liquefaction volume change using induced maximum excess pore pressure ratios with a sufficient degree of accuracy.

Shamoto *et al.* (1995a &1996a) show that the volume change after soil liquefaction can be uniquely related to "relative compression, Rc" regardless of type and density of sand, as defined by

$$Rc = \Delta e / (e_i - e_{min}) \ (\%) \quad (1)$$

in which e_i is the initial void ratio; e_{min} is the minimum void ratio; and Δe is the change in void ratio. In addition, they found that Rc could be a function of the maximum double amplitude of shear strain γ_{max} developed in the deposit during earthquake shaking, as shown in Fig.2. The data in the figure are based on tests on five sands with Dr ranging from 20% to 90%. The linear relationship between the two variables on the log-log chart leads to the following equation:

$$Rc = Ro\gamma_{max}{}^{n} \quad (2)$$

in which $n = 0.725$ and $Ro = 3.69$. Therefore, the post-liquefaction residual volumetric strain ε_{vr} may be determined by

$$\varepsilon_{vr} = \frac{\Delta e}{1+e_i} = R_o \frac{e_i - e_{\min}}{1+e_i} \gamma^n_{\max} \quad (3)$$

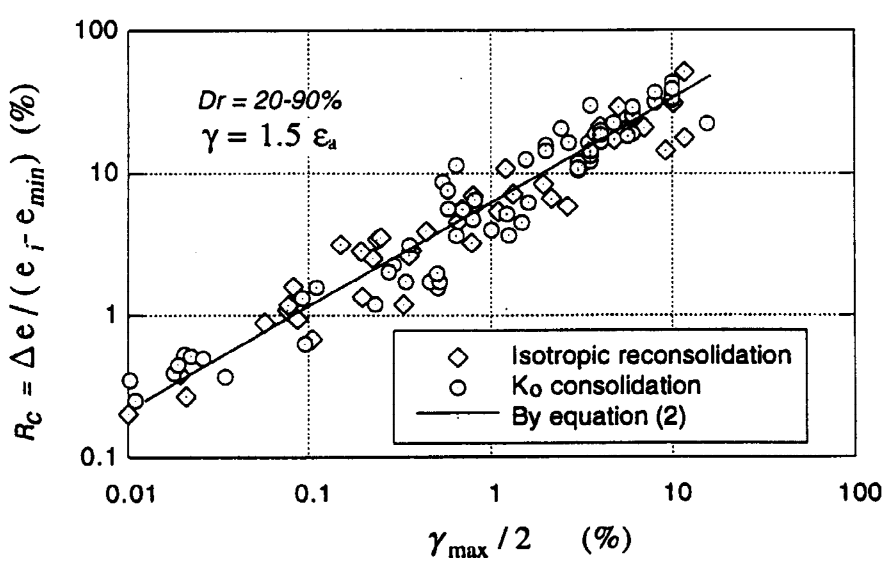

Fig.2 Relationship between relative compression and maximum double amplitude of shear strain for five sands over a wide density range (after Shamoto *et al.*, 1996a)

A great deal of laboratory experiments shows that large deformation always occurs after soil liquefaction. Especially it can develop when the effective confining stress reaches zero during undrained loading. In the case of cyclic undrained loading as shown in Fig. 3, with the development of induced γ_{max}, the effective stress becomes zero twice in one loading cycle. The stress-strain hysteresis curve in one loading cycle can be divided into two stress states, i.e., zero and non-zero effective confining stress states. The stress-strain hysteresis curves associated with non-zero effective stress states are similar in shape and thus are parallel to each other. This indicates that the changes in shear strain occurring during non-zero stress states are almost the same. Conversely, the shear strain induced at zero effective confining stress state increases with increasing number of load cycles. Therefore, the latter component of shear strain governs the increase in shear strain after initial liquefaction.

The above discussion implies that two shear strain components exist during post-liquefaction cyclic undrained loading. Thus, the post-liquefaction shear strain γ may be expressed as

$$\gamma = \gamma_d + \gamma_o \tag{4}$$

in which γ_d = shear strain component occurring during non-zero effective confining stress states and γ_o = shear strain component occurring during zero effective confining stress state.

A similar phenomenon can be also observed in monotonic undrained shear tests after complete or incomplete liquefaction, as shown in Fig.4. In this figure Curves-3 to 6 correspond to the cases after complete liquefaction, and Curves-1 and -2 to those after incomplete liquefaction. A comparison of Fig. 4 (a) with Fig. 4 (b) indicates that the shear strain values of different curves are quite different at the same shear stress level, although the corresponding effective stress paths almost coincide except for initial loading phases of Curves-1 and -2. It shows that two shear strain components stated above indeed exist also for monotonic undrained loading after initial liquefaction. Again, the shear strain component γ_o that occurs during zero effective confining stress state plays a decisive role in the development of large post-liquefaction shear strain.

On the basis of a new physical model of dilatancy, a relative compression concept, the theory of plasticity, and other previous available studies, Shamoto *et al.* (1995b) have presented new constitutive relations for the above post-liquefaction shear strains as follows:

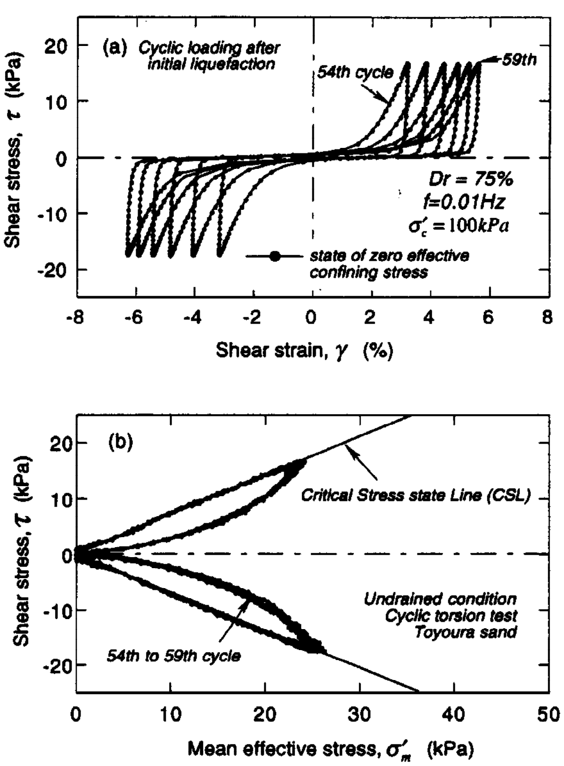

Fig.3 Two post-liquefaction shear strain components observed in a typical cyclic undrained torsion test

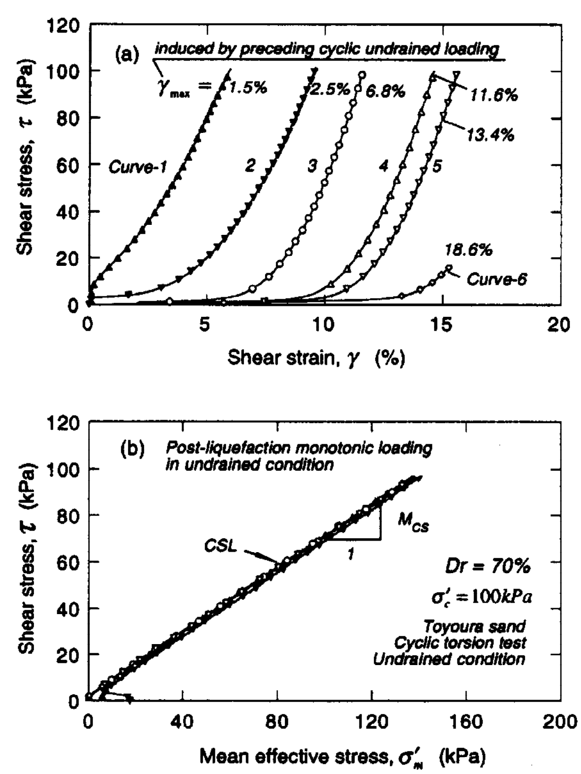

Fig.4 Two shear strain components observed in monotonic undrained torsion tests after incom plete and complete liquefaction

$$\gamma_o = \frac{R_o}{M_{CS}} \frac{e_o - e_{\min}}{1+e_o} (\gamma_{\max} - \gamma_{entry})^m \tag{5}$$

$$\gamma_d = \frac{\alpha K}{M_{cs} - M_o} (\frac{p'_i}{p_a})^A (\frac{M_{cs} q}{p'_i})^B \tag{6}$$

in which q and p' = current deviator and mean effective stresses; p_a = barometric pressure of $100kPa$; p'_i = initial effective confining pressure; M_{cs} and M_o = critical and phase transformation stress ratios defined respectively as $(q/p')_{cs}$ and $(q/p')_{PT}$ in undrained conditions, for example, M_{cs} = 1.20 and M_o = 0.93 for Toyoura sand with a relative density of 70%; m, Ro, α, A, B, and K = material constants determined by tests; and γ_{entry} is called "entrance shear strain" in double amplitude that triggers initial liquefaction. It may be determined by the following equation (Shamoto *et al.*, 1995b):

$$\gamma_{entry} = [-R_o \frac{e_o - e_{\min}}{1+e_o} \varepsilon_{vc.o}]^{1/m} \tag{7}$$

in which $\varepsilon_{vc.o}$ is volumetric strain due to reduction in p', ε_{vc}, at state of zero effective confining pressure, and takes the negative sign.

Based on Eq. (5) together with cyclic undrained torsion results of Toyoura sand, the relationship between preceding γ_{max} and current γ_o may be expressed in terms of the relationship between γ_{max} and $\gamma_o[M_{cs}(1+e_i)/(e_i-e_{min})]$, as shown in Fig. 5. In this figure the average γ_{entry}-value is 2.65% in the Dr range from 40% to 80%.

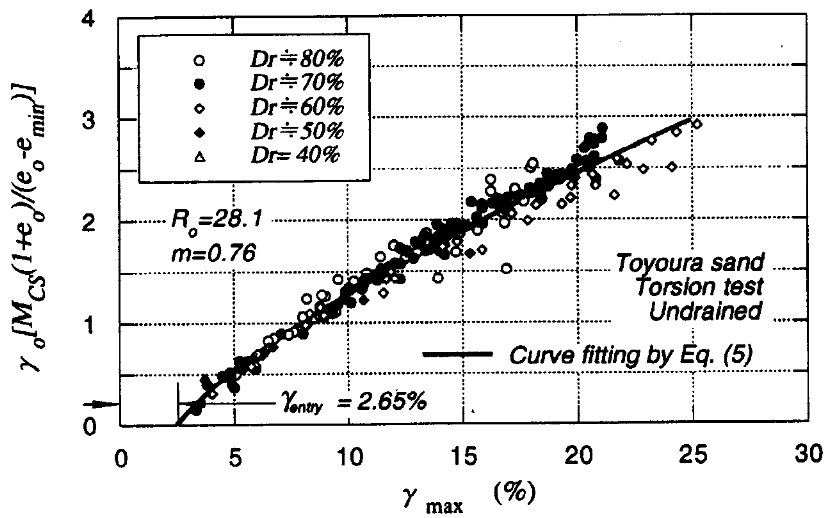

Fig.5 Effectiveness of equation (5) and determination of coefficients Ro and m (Shamoto *et al.*, 1995b)

ESTIMATION OF LIQUEFACTION-INDUCED MAXIMUM SHEAR STRAIN

Empirical Procedure of Estimation

On the basis of cyclic undrained triaxial tests on high-quality undisturbed sand samples, Tokimatsu & Yoshimi (1983) presented an empirical correlation of soil liquefaction in which dynamic shear stress ratio, τ_d/σ'_z, is expressed as a function of single amplitude of shear strain (= $\gamma_{max}/2$), and normalized SPT N_l-value adjusted in terms of fines content, N_a, as shown in Fig. 6. They also presented the following empirical equations for estimating τ_d/σ'_z, and N_a

$$N_a = \frac{170}{\sigma'_z + 70} N + \Delta N_f \tag{7}$$

$$\frac{\tau_d}{\sigma'_z} = 0.1(M-1) \frac{\alpha_{\max}}{g} \frac{\sigma_z}{\sigma'_z} (1 - 0.015z) \tag{8}$$

in which N = SPT N-value, z = depth in meters below ground surface, σ'_z is initial effective vertical stress in kPa at depth z, ΔN_f = a correction term for considering the influence of fines content F_c, τ_d is amplitude of uniform shear stress cycles equivalent to actual seismic shear stress time history, M = earthquake magnitude, α_{max} is maximum horizontal acceleration on the ground surface, and σ_z is initial vertical stress at depth z. ΔN_f is taken as being 0 for F_c < 5 %; (1.2 x F_c - 6) for 5 % < F_c <10 %; (0.2 x F_c + 4) for 10 % < F_c < 20 %; and (0.1 x F_c + 6) for 20 % < F_c < 50 %.

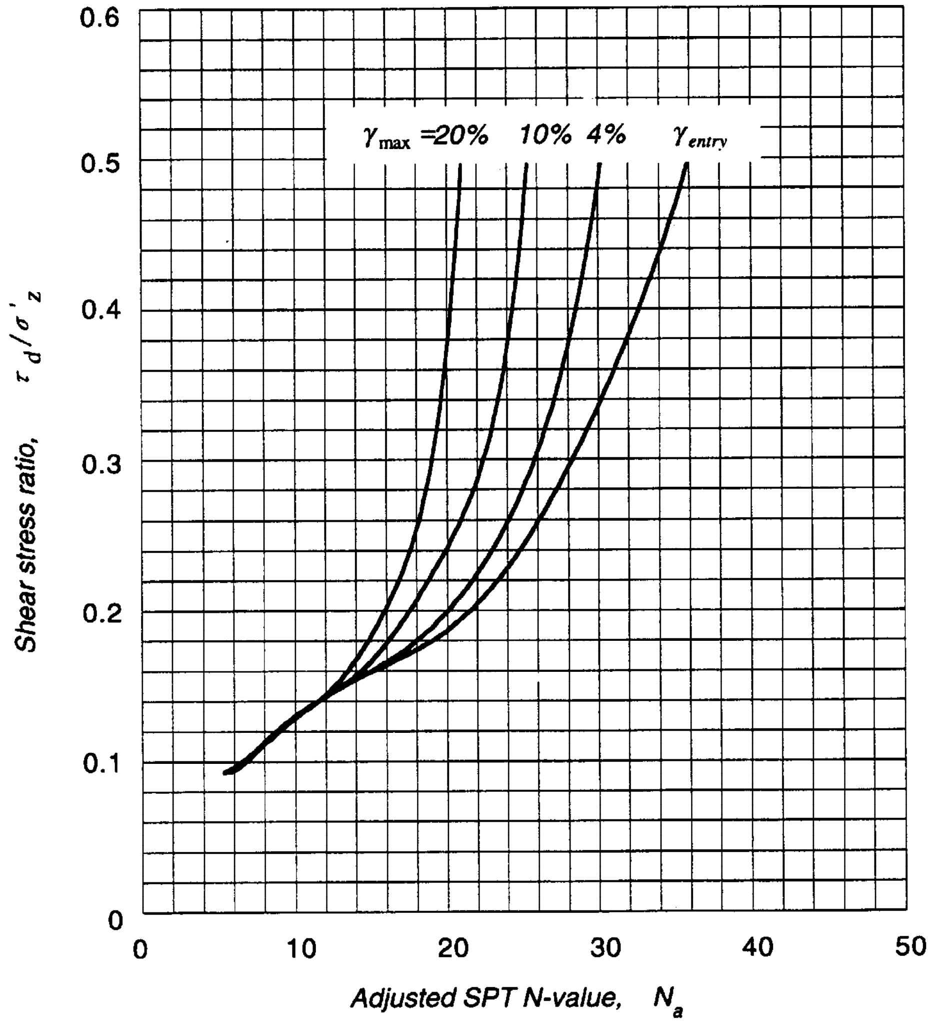

Fig.6 An empirical chart determining maximum double amplitude of shear strain induced by earthquake shaking (modified after Tokimatsu & Yoshimi, 1983)

The entrance shear strain γ_{entry} is also shown in Fig.6. The γ_{entry}-τ_d/σ'_z-N_a curve was defined based on equations (7), (8) and (9) as well as the test data for Toyoura sand conducted by the authors. Thus, the maximum double amplitude of shear strain γ_{max} may be estimated using the chart shown in Fig.6 and equations (8) and (9). Obviously, $\gamma_o = 0$ when $\gamma_{max} = \gamma_{entry}$.

Procedure of Estimation based on Effective Stress Analysis of Earthquake Response

The most rational way to determine the distribution of γ_{max} with depth in a deposit should be based on an effective stress response analysis. However, most of the effective stress-strain constitutive models currently available for the response analysis can evaluate the shear strain component γ_d only. The shear strain component γ_o, therefore, needs to be considered in the effective stress analysis of a soil deposit.

Figs. 7 (a) and (b) show time histories of the shear stress ratio τ/σ'_c and shear strain γ measured in a cyclic drained torsion test. The measured γ was separated into γ_d and γ_o, and are plotted in Figs. 7(c) and (d). If γ_d-value was known and if $\gamma_d > \gamma_{entry}$, γ_o could be calculated by Eq. (5), as shown in Fig. 7(d) with the dotted curve. The good agreement between the tested and calculated γ_o-values suggests that this method of calculation is suitable for determining the shear strains induced by both post-liquefaction cyclic and monotonic loading. Thus, one can use the effective stress response analysis to determine the time history of γ_d at any depth in a deposit, and then, use this method to determine the corresponding changes in post-liquefaction shear strain $\gamma (= \gamma_d + \gamma_o)$.

Estimation of Permanent Deformation in Saturated Level Ground

(1) Estimation of settlement of ground surface. According to the experimental results shown in Fig. 2, the settlements of saturated sandy deposits with level ground due to earthquake shaking may be estimated by the following procedure: a) Determine the variation of e_i and e_{min} with depth of a deposit using the empirical relations:

$$D_r = 16\sqrt{N_a} \tag{10}$$

$$e_{\max} = 0.02 \times F_c + 1.0 \tag{11}$$

$$e_{\min} = 0.008 \times F_c + 0.6 \tag{12}$$

$$e_i = e_{\max} - (e_{\max} - e_{\min}) \times D_r \tag{13}$$

Eq. (10) and Eqs. (11) and (12) are, respectively, proposed by Tokimatsu & Yoshimi (1982) and Hirama (1991); b) Estimate the distribution of γ_{max} with depth using the method proposed in this study; c) Calculate the distribution of ε_{vr} with depth by equation (3) and then determine the settlement of ground surface, D_s by

$$D_s = \sum_{j=1}^{N} (\varepsilon_{vr})_j \Delta z_j = \sum_{j=1}^{N} R_o \cdot \left(\frac{e_i - e_{\min}}{1 + e_i}\right)_j (\gamma^n_{\max})_j \Delta z_j \tag{14}$$

in which N is the total number of the divided layers and Δz_j is the thickness of the j th layer.

Fig. 8 shows the boring log of a saturated sand deposit whose total ground settlement amounted to about 44 *cm* during the 1995 Hyogoken-Nanbu earthquake. The distribution of accumulated settlement from the depth of about 16 *m* to the ground surface, for any α_{max}, may be evaluated by the above procedure, as shown in Fig.8. The calculated total ground settlement reaches 46*cm* to 49*cm* for the maximum accelerations of 300-400*Gal* probably developed during the earthquake, showing good agreement with the observed value. This indicates that the proposed method is effective.

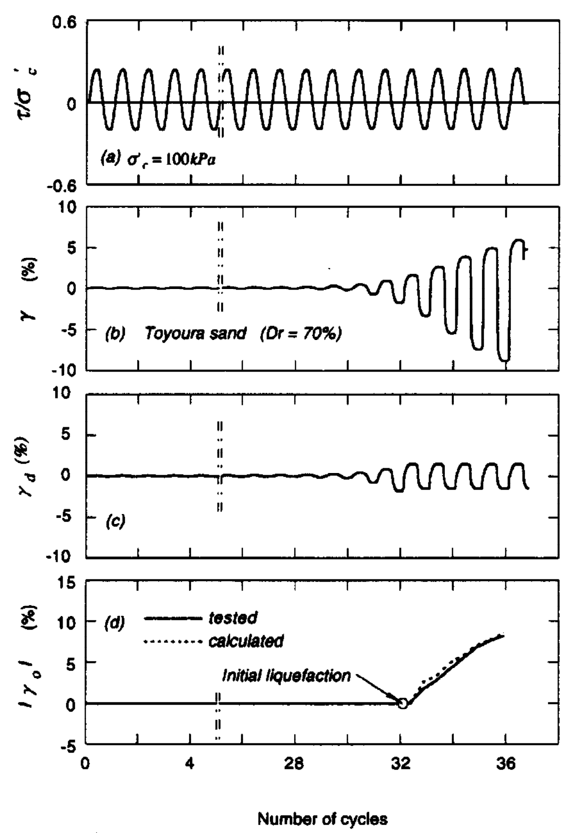

Fig.7 Principle estimating two post-liquefaction shear strain components based on an undrained cyclic torsion test result

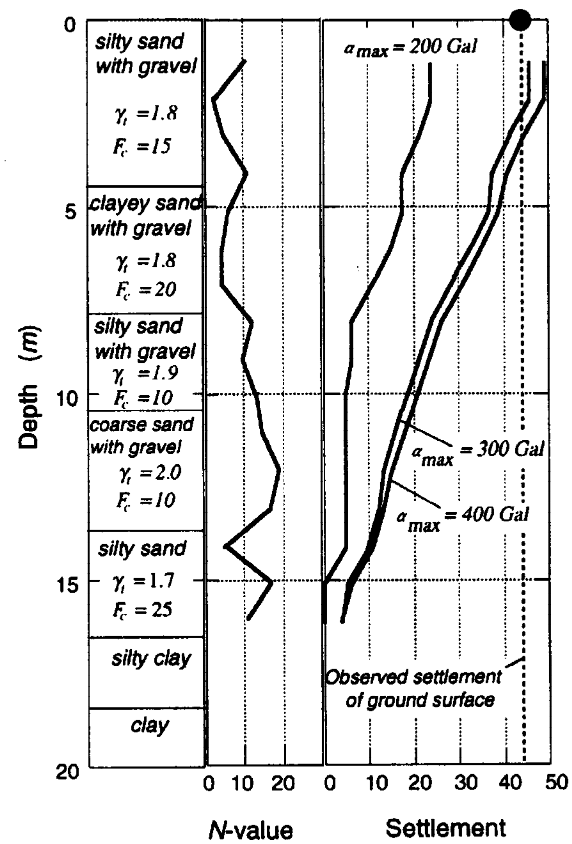

Fig.8 Comparison of the estimating ground settlements with the result observed during the 1995 Hyogo-ken Nanbu earthquake

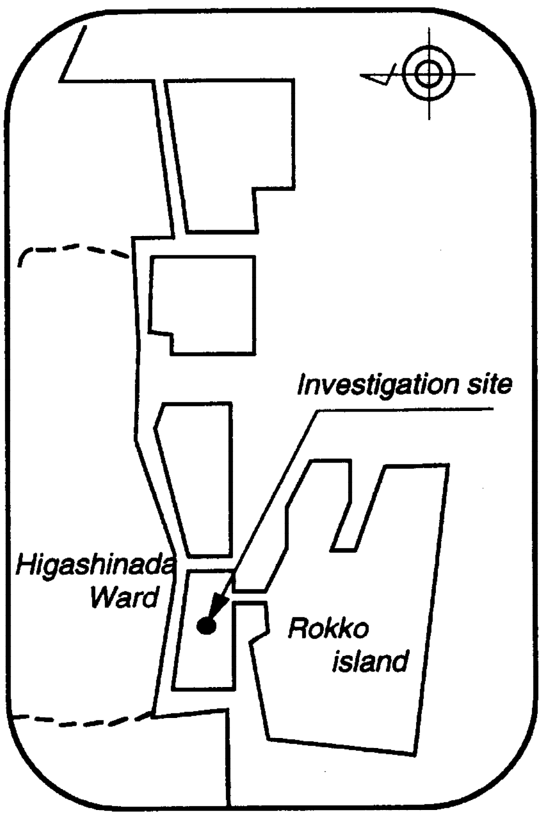

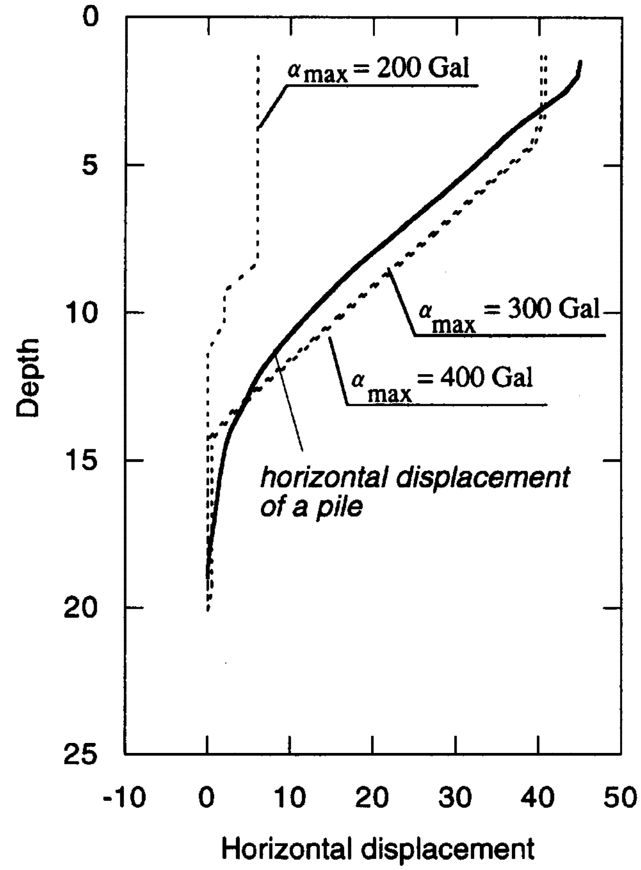

Fig.9 Location of site investigation

Fig.10 Comparison of the estimating horizontal ground displacements with the result observed during the 1995 Hyogo-ken Nanbu earthquake (Shamoto *et al.*, 1996b)

(2) Estimation of Horizontal Displacement. Large lateral permanent displacements occurred in sandy soil deposits with nearly level ground surfaces during the past strong earthquakes (e.g., Hamada *et al.*, 1986). A site investigation was conducted on pile foundations of three- and four-story buildings which settled and tilted due to soil liquefaction during the 1995 Hyogo-ken Nanbu earthquake (Shamoto *et al.*, 1996b). The site is located at the reclaimed level deposit in Sumiyoshihama island and is about 250 m away from the nearest wall, as shown in Fig. 9. The fill consists mainly of sandy soils (D_{50} =0.9 mm and F_c = 15 %) down to a depth of 13 m from the ground surface. Based on the the analysis of the investigation results, it is found that 1) lateral permanent ground displacement occurred due to liquefaction; and 2) horizontal displacements of piles were governed by post-liquefaction lateral displacements of the surrounding liquefied soil, and particularly for the cases of the investigated buildings, the horizontal displacement was almost consistent with that of the deposit. The solid curve in Fig.10 is the distribution of the measured horizontal displacements of a pile of the building investigated.

The major cause of the large lateral ground displacements that occurred in level ground is unclear; however, it may be explained as a consequence of the induced post-liquefaction shear strain component γ_o. Based on such an opinion, the permanent ground displacement due to post-liquefaction shear strain component γ_o is estimated for this case history. The corresponding soil parameters used for the estimation may be seen in the reference by Shamoto *et al.* (1996b). The α_{max}-values of 200Gal, 300Gal, and 400Gal are assumed. For one given α_{max}-value, the distribution of γ_{max}-value with depth was estimated by equations (7) and (8) and with the chart shown in Fig. 6. The corresponding γ_o-values were then determined by equation (5). In the case of level ground, γ_o is the maximum prossible shear strain after liquefaction since γ_d = 0 after an earthquake. Also shown in Fig. 10 with the dotted curves is the distribution of horizontal displacement with depth thus estimated for three α_{max} levels. It is seen that, for the cases of α_{max} = 300 and 400Gal, the estimated horizontal permanent displacements are comparable with the observed value, and their distribution with depth is almost consistent with the observed pile displacement. This suggests that the proposed method is effective as a first approximation for predicting post-liquefaction lateral permanent deformation of level ground.

Estimation of Permanent Ground Deformation in 2-D & 3-D Problems

Permanent ground deformation may occur in a deposit with inclined surface or near quay walls, which is usually regarded as two- and three-dimensional boundary-value problems. Based on the method to determine γ_o cited above, a method to predict permanent ground deformation in two- and three-dimensional problems may be suggested as follows:

a) Determine γ_{max} of each soil element in the deposit considered, using the method proposed in this study, and determine the volumetric strain ε_v and the shear strain component γ_o ;

b) Determine the initial condition of calculation, including mean effective principal stress $\sigma'_{m,o}$, initial shear stress to, and shear strain component $\gamma_{d,o}$ of each element, using the equivalent linear analysis for gravitational force field;

c) Calculate the equivalent shear modulus G_{eq} of each element, using:

$$G_{eq},_i = \tau_{i-1} /(\gamma_o + \gamma_{d,i-1}) \tag{15}$$

in which i is iteration number. Obviously, $G_{eq},_1 = \tau_o /(\gamma_o + \gamma_{d,o})$ at $i = 1$.

d) Calculate the equivalent bulk modulus K_{eq} of each element using:

$$K_{eq},_i = \sigma'_{m},_{i-1} / \varepsilon_v \tag{16}$$

e) Perform the equivalent linear analysis for gravitational force field, based on the calculated G_{eq}- and K_{eq}- values, and obtain $\tau_{d,i}$, $\gamma_{d,i}$, and $\sigma'_{m,i}$ of each element;

f) Repeat steps c) to e) until the difference in shear strain, $\Delta\gamma_d = (\gamma_{d,i} - \gamma_{d,i-1})$, becomes negligibly small.

The application of the above procedures to actual boundary-value problems will be introduced in the other report due to the limited length of this paper.

CONCLUSIONS

Post-liquefaction permanent deformation in saturated sandy soil is a result of the induced volumetric and deviator changes induced in the soil subjected to cyclic or monotonic loading applications. A new approach to predict post-liquefaction settlement and lateral displacement has been established based on several new experimental facts and findings. It has been confirmed that the proposed method may be used as a first approximation for estimating large post-liquefaction ground deformation induced by earthquake shaking.

REFERENCE

Hamada, M., Yasuda, S., Isoyama, R. and Emoto, K.(1986):"Study on liquefaction induced permanent ground displacements," *Association for the Development of Earthquake Prediction,* Japan, pp.1-87.

Hirama, K. (1981): " Several private opinions on adaptability of relative density," *Proceedings, Symposium on sand relative density and its engineering property*, JSSMFE, pp. 53-56 (in Japanese).

Ishihara, K. and Yoshimine, M.(1993): "Evaluation of settlements in sand deposits following liquefaction during earthquakes," *Soils and Foundations*, Vol. 32, No. 1, pp. 173-188.

Seed, H.B. and Lee, K.L. (1966):" Liquefaction of saturated sands during cyclic loading, " *Journal of the Soil Mechanics and Foundation Engineering Division,* ASCE, Vol.92, No.SM6, pp.105-134.

Shamoto, Y., Sato, M. and Zhang, J.-M. (1995a): " Liquefaction-induced settlements in sand deposits," *Proceedings, Third International Conference on Recent Advances in Geotechnical Earthquake Engineering and Soil Dynamics,* Vol. II, pp. 215-220.

Shamoto, Y., Zhang, J.-M. and Goto, S.(1995b): " Mechanism of large post-liquefaction deformation in saturated sand," to be submitted to *Soils and Foundations* in November, 1995.

Shamoto, Y., Sato, M. and Zhang, J.-M.(1996a): "Simplified Estimation of Earthquake-induced settlements in Saturated sand deposits," *Soils and Foundations,* Vol.36, No.1.

Shamoto, Y., Sato, M., Futaki, M., and Shimazu, S.(1996b): " A site investigation of post-liquefaction lateral displacements of pile foundations in reclaimed land," *Tsuti-to-Kiso*, Vol. 44, No.3 (in Japanese).

Tokimatsu, K. and Yoshimi, Y. (1983): " Empirical correlation of soil liquefaction based on SPT *N*-value and fines content," *Soils and Foundations*, Vol. 23, No. 4, pp. 56-74.

Tokimatsu, K. and Seed, H.B.(1987): "Evaluation of settlements in sands due to earthquake shaking," *Journal of Geotechnical Engineering Division,* Vol. 113, No. 8, pp. 861-878.